*Pharmaceutical Research, Vol. 23, No. 6, June 2006 (© 2006)*
DOI: 10.1007/s11095-006-0082-3

*Research Paper*

# A Specific Picomolar Hybridization-Based ELISA Assay for the Determination of Phosphorothioate Oligonucleotides in Plasma and Cellular Matrices

**Xiaohui Wei,[1] Guowei Dai,[1] Guido Marcucci,[2,3] Zhongfa Liu,[1] Dale Hoyt,[4] William Blum,[3] and Kenneth K. Chan[1,2,5]**

*Received December 20, 2005; accepted January 20, 2006*

***Purpose.*** To develop and validate an ultrasensitive and specific hybridization-based enzyme-linked immunosorbent assay method for quantification of two phosphorothioate oligonucleotides (PS ODNs) (G3139 and GTI-2040) in biological fluids.
***Methods.*** This assay was based on hybridization of analytes to the biotin-labeled capture ODNs followed by ligation with digoxigenin-labeled detection ODN. The bound duplex was then detected by anti-digoxigenin-alkaline phosphatase using Attophos® (Promega, Madison, WI, USA) as substrate. S1 nuclease and major factors such as the hybridization temperature, concentration of capture probe, and the use of detergent were evaluated toward assay sensitivity, selectivity, and accuracy.
***Results.*** The method is selective to the parent drugs with minimal cross-reactivity (<6%) with 3′-end deletion oligomers for both G3139 and GTI-2040. A linear range of 0.05 to 10 nM ($r^2 > 0.99$) was observed for GTI-2040 in a variety of biological matrices. For both G3139 and GTI-2040, the within-day precision and accuracy values were found to be <20% and 90–110%, respectively; the between-day precision and accuracy were determined to be <20% and 90–120%. Addition of S1 nuclease combined with washing step greatly improved the assay linearity and selectivity. The utility of this assay was demonstrated by simultaneous determination of GTI-2040 in plasma and its intracellular levels in treated acute myeloid leukemia patients.
***Conclusions.*** The validated hybridization enzyme-linked immunosorbent assay method is specific for quantitation of PS ODNs in biological samples to picomolar level. This method provides a powerful technique to evaluate plasma pharmacokinetics and intracellular uptake of PS ODNs in patients and shows its utility in clinical evaluations.

**KEY WORDS:** hybridization–ligation ELISA; intracellular drug level; pharmacokinetics; phosphorothioate oligonucleotides.

[1] Division of Pharmaceutics, College of Pharmacy, The Ohio State University, Columbus, Ohio 43210, USA.
[2] The Comprehensive Cancer Center, Rm 308 OSU CCC, The Ohio State University, 410 West 12th Ave, Columbus, Ohio 43210, USA.
[3] Division of Hematology-Oncology, College of Medicine and Public Health, The Ohio State University, Columbus, Ohio 43210, USA.
[4] Division of Pharmacology, College of Pharmacy, The Ohio State University, Columbus, Ohio 43210, USA.
[5] To whom correspondence should be addressed. (e-mail: chan.56@osu.edu)

**ABBREVIATIONS:** AML, acute myeloid leukemia; AP, alkaline phosphatase; AS ODN, antisense oligonucleotide; AUC, area under the curve; BM, bone marrow; CL, total body clearance; $C_{ss}$, steady state concentration; CV, coefficient of variation; Dig, digoxigenin; ELISA, enzyme-linked immunosorbent assay; LLOQ, lower limit of quantification; LOD, limit of detection; mRNA, messenger ribonucleic acid; PBMC, peripheral blood mononuclear cell; PD, pharmacodynamics; PK, pharmacokinetics; PS ODN, phosphorothioate oligonucleotide; RBC, red blood cells; RNase H, ribonuclease H; RNR, ribonucleotide reductase.

## INTRODUCTION

Nucleic acid hybridization has long been known to play a vital role in biological processes, and its precise complementary association with messenger ribonucleic acid (mRNA) has recently been recognized as a potential therapeutic strategy. Specific segments of DNA-like or modified DNA known as antisense oligonucleotides (AS ODNs) capable of hybridizing with specific mRNA or regions of mRNA have now been developed to aim at disruption of the expression of genes that associate with malignancy transformation. Thus, antisense oligonucleotides inhibit processing or translation of its target mRNA to proteins. The native phosphodiester oligonucleotides suffer from low *in vitro* and *in vivo* stability and did not achieve significant therapeutic expectation. On the other hand, the first generation of antisense compounds, such as phosphorothioate oligonucleotides (PS ODNs), offer significantly improved stability and biological activities, and

several are now being evaluated clinically in various molecular targets including cancer, viral diseases, and inflammatory disorders (1–6). To date, there are over 20 ongoing clinical trials testing antisense compounds. PS ODNs possess favorable nuclease resistance and ribonuclease H (RNase H) activation properties and demonstrate clinical responses, acceptable toxicity, and thus, clinical significance (4–6).

GTI-2040, a 20-mer PS ODN complementary to the mRNA of the R2 subunit of ribonucleotide reductase (RNR), has demonstrated down-regulation effects on mRNA and protein levels of R2 in several human tumor cell lines in a sequence- and target-specific manner (7). In nude and severe combined immunodeficient (SCID) mice, GTI-2040 significantly inhibits growth of a wide range of xenografted human tumors (7). Results from the phase I clinical studies of GTI-2040 on advanced solid tumors showed that GTI-2040 has manageable toxicity profile and is well tolerated as a single agent (8). This agent is currently undergoing clinical evaluation in patients with acute myeloid leukemia (AML) in combination with high-dose cytarabine at the James Comprehensive Cancer Center and Solove Research Institute at The Ohio State University.

Another PS ODN, G3139, an 18-mer antiapoptotic protein Bcl-2 antisense, has shown a response rate of 45% and target down-regulation in approximately 75% of patients with refractory or relapsed AML in one of our initial phase I clinical trials (9,10). Based on the promising clinical response, G3139 is currently being evaluated in several phase I to III trials for both solid tumors and hematological malignancies.

To support the clinical evaluation of pharmacokinetic behaviors of antisense drugs and its relationship with efficacy, toxicity, and disease response, it is essential to develop a specific, sensitive, and accurate quantification method of these agents in biological matrices. Conventional approaches, including anion-exchange high-performance liquid chromatography (HPLC), liquid chromatography/mass spectrometry (LC/MS), capillary gel electrophoresis (CGE), and chromatography of radiolabeled oligonucleotides, have been used in biological sample analysis (11–18). However, insufficient sensitivity [lower limit of quantification (LLOQ) >10 nM] and/or lack of selectivity toward metabolites has compromised their ability to either fully characterize the plasma pharmacokinetics or measure intracellular drug concentrations, which may reveal its relationship with the target intervention [pharmacokinetics (PK)/pharmacodynamics (PD)], after drug administration (19,20). Moreover, these methods demand extensive sample preparation prior to analysis and may be subjected to matrix effects. More recently, hybridization between two single-strand oligonucleotides has attracted considerable attention in their isolation and analysis based on the specific high binding affinity of nucleotide base pairing. Coupled with enzyme-linked immunoreaction, pM levels assay sensitivity could be achieved. Thus, hybridization-based assays were proposed as quantification methods for antisense ODNs, and a number of template designs have been reported for polynucleotide drugs including PS ODNs and ribozymes (19–25). Among them, a one-step homogeneous competitive hybridization method showed good sensitivity, but its inability to differentiate from metabolites (48% cross-reactivity with the 3′N-2) limits its extensive use (21). In a more recent hybridization assay, a capture probe design using a locked nucleic acid without 5′ overhang showed superb assay sensitivity in the femtomole range, but the assay was still unable to distinguish the parent drug from chain-shortened oligomers (22). We and the others have shown that the hybridization–ligation-based enzyme-linked immunosorbent assay (ELISA) for the analysis of PS ODNs could be rendered highly specific by using a capture probe with a 5′ overhang for isolation and a detection probe for signaling (10,20,24). In addition, this method provided good accuracy, wide range of linearity, and high throughput with minimal sample clean-up and was used in pharmacokinetic studies of two antisense ODNs (10,19,20). However, very few of these reports investigated factors that influence the assay and those that did only had limited information.

In this paper, we further refined this hybridization procedure by examining in detail the major factors that can be optimized and aimed to describe a general method for a two-step noncompetitive hybridization–ligation ELISA method for PS ODNs. Two examples of application, one refinement of the previous assay for the Bcl-2 antisense G3139 and a newly validated assay for GTI-2040 in several biological matrices, were provided, and initial clinical pharmacokinetic data of GTI-2040 were also described.

## MATERIALS AND METHODS

### Antisense and Reagents

The 20-mer PS ODN, GTI-2040, with sequence of 5′-GGC TAA ATC GCT CCA CCA AG-3′, and the 18-mer PS ODN, G3139, with sequence of 5′-TCT CCC AGC GTG CGC CAT-3′, were provided by the National Cancer Institute (Bethesda, MD, USA) and used without further purification. Both the 3′-end (3′N-1, 3′N-2, 3′N-3) and the 5′-end (5′ N-1, 5′ N-2, 5′ N-3) putative metabolites of GTI-2040 and G3139 were purchased from Integrated DNA Technologies (Coralville, IA, USA). The scrambled control oligomer of GTI-2040 (5′-ACG CAC TCA GCT AGT GAC CA-3′), mismatched GTI-2040 (5′-ACG CAC TCA GCT AGT GAC CA-3′), reversed G3139 (TCT CCC AGC GTG CGC CAT), and mismatched G3139 (TCT CCC AGC ATG TGC CAT) were all obtained from Integrated DNA Technologies. The purity and identity of each oligomer were verified by HPLC/UV/MS (ion trap mass spectrometer model LCQ, Finnigan, San Jose, CA, USA). The capture probe for the one-step hybridization method of GTI-2040 was synthesized as a 3′-end biotin attached and 5′-end digoxigenin (Dig) attached 20-mer DNA with sequence complementary to GTI-2040. The capture probe for GTI-2040 used in two-step hybridization ELISA was designed as a 29-mer DNA oligonucleotide with the first 20-mer sequence from the 3′-end complementary to GTI-2040. The 3′-end was attached to a NeutrAvidin-coated 96-well plate via biotin, and the 9-mer overhang (5′-TAA CTA GTG-3′) served as a template for the detection probe. The capture probe used for G3139 was designed as a 27-mer DNA oligonucleotide with sequence complementary to G3139 from the 3′-end followed by nine additional nucleotides (sequence 5′-TCG CTA TTC-3′) at the 5′-end and with biotin attached at the 3′-end. A 9-mer DNA with phosphate at the

5′-end and digoxigenin at the 3′-end with sequence complementary to the 5′-end 9-mer overhang of the capture probes of GTI-2040 or G3139 is used as an appropriate detection probe for the hybridization–ligation ELISA assay. All of these probes were custom-synthesized by Integrated DNA Technologies.

Reacti-Bind NeutrAvidin-coated polystyrene plates were purchased from Pierce (Rockford, IL, USA). GTI-2040 and G3139 standards were diluted in TE [Tris–HCl and ethylenediaminetetraacetic acid (EDTA)] buffer containing 10 mM Tris–HCl and 1 mM EDTA (pH = 8.0). The hybridization buffer used in preparation of capture probe solution contained 60 mM sodium phosphate, pH 7.4, 1.0 M NaCl, 5 mM EDTA, and 0.2% Tween 20. The ligation buffer was prepared as a mixture of 66 mM Tris–HCl, pH 7.6, 10 mM $MgCl_2$, 10 mM DTT, 1 mM ATP, 5 U $mL^{-1}$ T4 DNA ligase, and 100 nM detection probe oligonucleotide. T4 DNA ligase and ATP were purchased from Amersham Biosciences (Piscataway, NJ, USA). The washing buffer used throughout the assay contained 25 mM Tris–HCl, pH = 7.2, 0.15 M NaCl, and 0.2% Tween 20. The anti-digoxigenin-alkaline phosphatase (AP) was obtained from Roche (Indianapolis, IN, USA). Attophos® and its reconstitution solution were purchased from Promega (Madison, WI, USA). Blank human plasma was obtained from Red Cross (Columbus, OH, USA). Detection was accomplished using a Gemini XS plate reader (Molecular Devices, Sunnyvale, CA, USA).

## Hybridization ELISA Assay Procedures

### *A One-Step Hybridization ELISA*

The principle of a one-step hybridization ELISA is shown in Scheme 1A. Basically, the capture and detection of the analyte was accomplished on a one-strand capture probe, which is complementary to the analyte without an overhang and contains biotin at the 3′-end and digoxigenin at

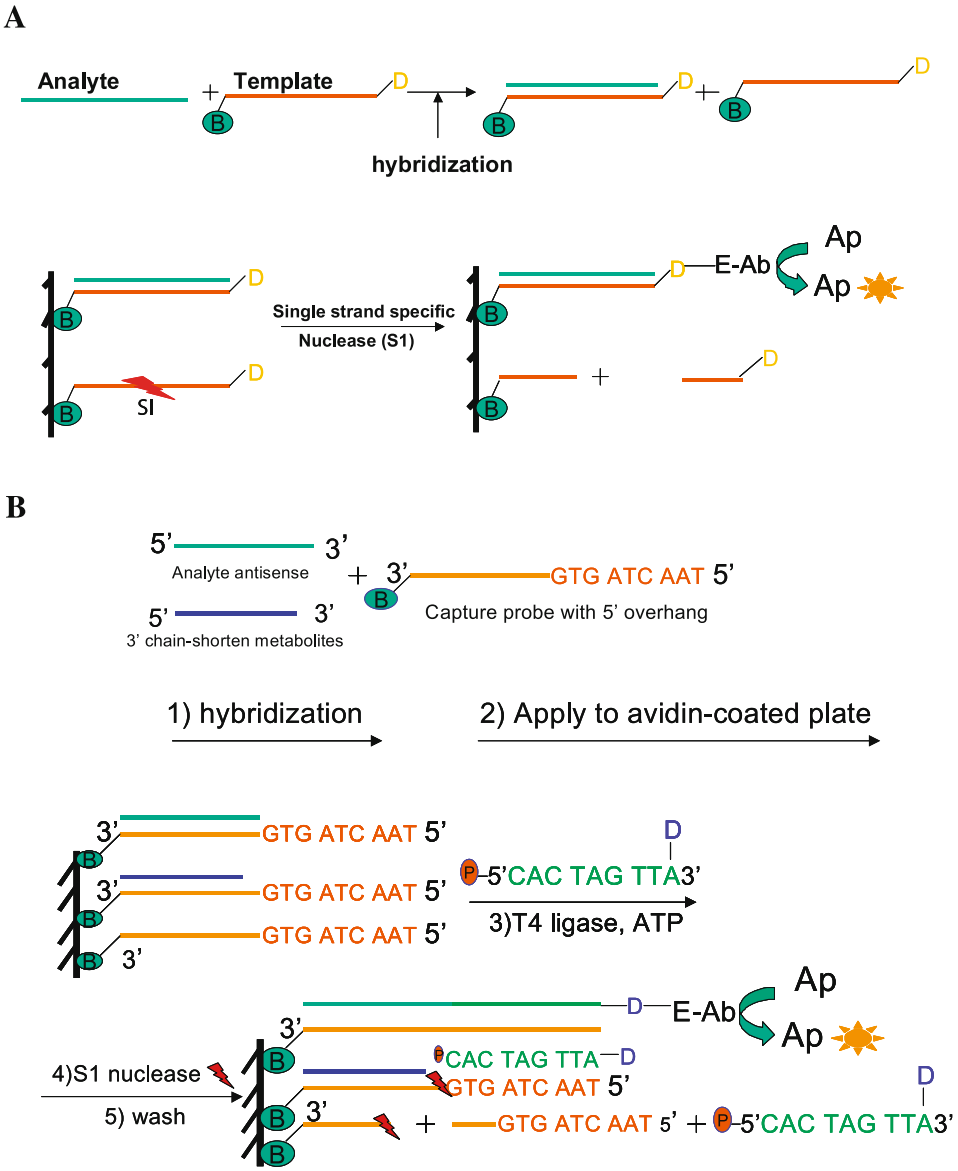


**Scheme 1.** Illustrations of hybridization ELISA. (A) A one-step hybridization ELISA. (B) A two-step hybridization–ligation ELISA.

the 5′-end. After analyte capture probe hybridization and the attachment of the duplex to the 96-well plate, S1 nuclease was added, followed by a 2-h incubation at 37°C. Then anti-digoxigenin-AP with super bovine serum albumin (BSA) block buffer was added into the wells, followed by incubation for 0.5 h at room temperature. After washing, an appropriate volume of Attophos substrate solution in diethanolamine buffer was added into each well and the plate was incubated at 37°C for 0.5 h. Attosphos substrate solution with low fluorescence was cleaved by the conjugated alkaline phosphatase to form a highly fluorescent product. The generated fluorescence was measured at Ex 430/Em 560 (filter = 550 nm) using a Gemini XS fluorescence microtiter plate reader (Molecular Devices).

*A Two-Step Hybridization–Ligation ELISA Assay*

The hybridization–ligation ELISA principle is shown in Scheme 1B. This method is based on a two-step hybridization, first by base pairing of analytes to the capture probe with an overhang, followed by hybridization with a detection probe, which is ligated to the analyte. The detail of the procedure is described in Scheme 2. Basically, 200 nM capture probe in hybridization buffer solution was first heated at 95°C for 5 min in a heating block (Van Water and Rogers, Coraopolis, PA, USA) to disrupt the possible secondary structure. Then 100 μL of the capture probe solution was added to 100 μL plasma or other biological matrices containing GTI-2040 or G3139, and the solution was mixed in a polypropylene 96-well plate. Five microliters of 10% Triton X-100 was added to the hybrid complex to a final concentration of 0.25% of Triton X-100. The mixture was incubated at 42°C for 2.5 h for hybridization. Then 150 μL of the solution was transferred to a NeutrAvidin-coated 96-well plate, which was incubated at 37°C for 30 min to allow the attachment of biotin labeled capture probe to NeutrAvidin-coated wells. The plate was washed six times with washing buffer, and 150 μL ligation solution containing 5 U $mL^{-1}$ T4 DNA ligase and 100 nM detection probe was added to each well. The plate was incubated overnight at 18°C. The plate was washed three times with washing buffer and three times with HPLC water to remove the unligated detection probe. Following addition of 60 U per well S1 nuclease solution in 100 mM NaCl, the plate was incubated at 37°C for 2 h to cleave the truncated duplex. After washing six times, the plate was blocked with 1:1 Superblock buffer in Tris buffered saline (TBS; Pierce). Then 150 μL anti-digoxigenin-AP diluted with 1:2500 super BSA block buffer in TBS (Roche, Mannheim, Germany) was added into each well, followed by incubation for 0.5 h at room temperature with gentle shaking. After washing six times, 150 μL substrate solution (36 mg Attophos in 60 mL diethanolamine buffer) was added into each well, and the plate was incubated at 37°C for 30 min. Finally, fluorescence intensity was measured at Ex 430/Em 560 (filter = 550 nm) using a Gemini XS fluorescence microtiter plate reader (Molecular Devices).

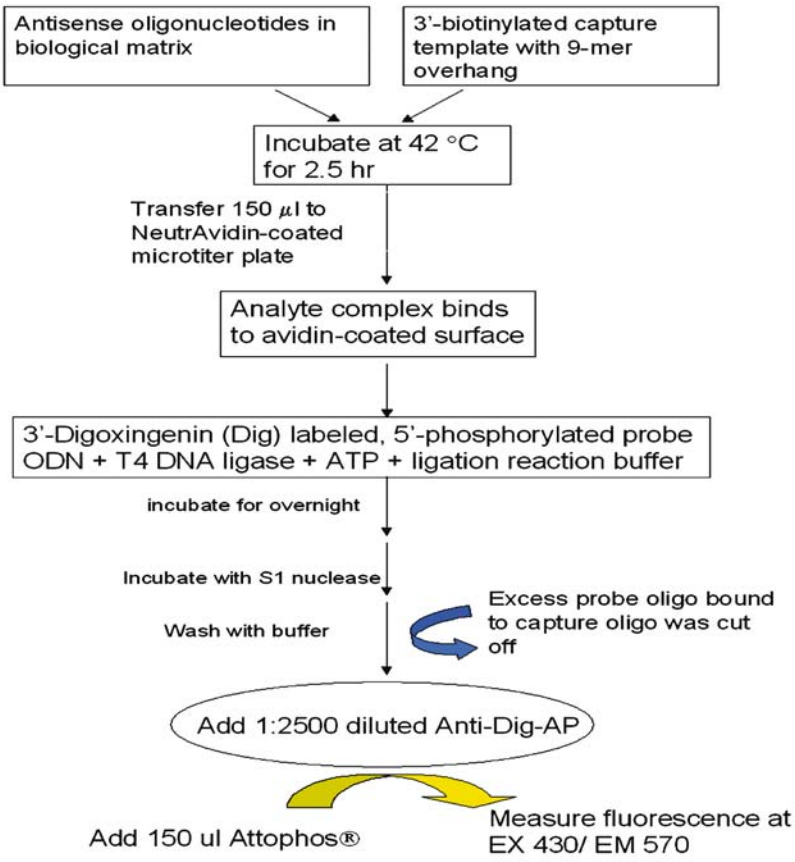


**Scheme 2.** The working procedure of hybridization ELISA assay to measure antisense drugs in plasma and cell lysate.

### Evaluation of Cutting Efficiency of S1 Nuclease

The one-step hybridization ELISA was used to evaluate the cutting efficiency of S1 nuclease, and GTI-2040 was used for evaluation. A control standard curve of fluorescence response *vs* concentration of intact one-step capture ODN in human plasma was first established as follows. To each of 100 μL standard solutions containing one-step capture ODN of GTI-2040 at 0.025, 0.050, 0.1, 0.2, 0.5, 1, 2, 5, 10, 20, and 50 nM, 100 μL of hybridization buffer was added, and the solution was incubated for 2.5 h at 42°C. Then, 150 μL of mixture was transferred into a NeutrAvidin-coated 96-well plate, which was incubated at 37°C for 0.5 h, facilitating biotin–avidin binding. After incubation with 100 mM NaCl solution for 2 h at 37°C, the plate was treated with anti-Dig-AP antibody, followed by the addition of Attophos substrate with a washing step between each steps, as described in the assay procedure of a one-step hybridization ELISA. Fluorescent response from the one-step template ODN of GTI-2040 was then measured. The standard curve of fluorescence responses vs concentrations of digoxigenin-labeled one-step capture ODN was established, and the linear regression equation was obtained.

Cutting efficiencies at two levels of S1 nuclease, namely, 60 and 100 U per well, were evaluated on each of four concentrations of one-step ODN, i.e., 50, 100, 200, and 250 nM. The procedure was the same as above except that 100 mM NaCl solution was replaced by 60 or 100 U per well of S1 nuclease in 100 mM NaCl solution. The remaining concentrations of one-step capture ODN after the treatment with S1 nuclease were measured and calculated from the regression equation derived from the standard curve. The level of one-step capture ODN cleaved by S1 nuclease was thus obtained by subtracting the residual concentration of the capture ODN from the initial values. The cutting efficiency of S1 nuclease on GTI-2040 one-step capture ODN was calculated as:

$$\textit{Cutting efficiency}(\%) = \frac{\textit{Added concentration of captureODN} - \textit{Measured concentration of captureODN}}{\textit{Added concentration of capture ODN}} \times 100\% \quad (1)$$

### Selectivity of Hybridization–Ligation ELISA

#### *Effect of S1 Nuclease on the Assay Selectivity*

Effect of S1 nuclease on cross-reactivity of the 3′N-1 metabolite toward GTI-2040 in hybridization–ligation ELISA was evaluated at the concentration range of GTI-2040 from 0.1 to 500 nM in human plasma. Four levels of S1 nuclease in addition to the blank, i.e., 0, 15, 30, 60, 100 U per well, were used for evaluation of its optimal level. Procedure for hybridization–ligation ELISA was described previously.

#### *Specificity and Selectivity of Hybridization–Ligation ELISA*

Using 60 U per well S1 nuclease, cross-reactivity of 3′-end metabolites, 5′N-1, and control oligomers (scrambled or mismatched oligonucleotides) on GTI-2040 at the concentration range between 50 pM and 1 μM in 10% human plasma in TE buffer was evaluated. The observed cross-reactivity profiles of these oligonucleotides were compared with those of the parent drugs. The cross-reactivity of each metabolite toward GTI-2040 was determined as the percentage of their $E_{max}$ values to that of GTI-2040. The $E_{max}$ values were calculated by nonlinear regression model in SigmaPlot (SPSS, Chicago, IL, USA).

### Method Validation

The hybridization–ligation ELISA method for GTI-2040 in human plasma, red blood cells (RBC), urine, and K562 cell lysate was validated. Linearity at the concentration range between 50 and 10,000 pM was evaluated for both analytes in 10% human and 10% mouse plasma in TE buffer, 100% human plasma, and K562 cell lysates. Within-day and between-day accuracy and precision were determined at 100 pM [low quality control (QC)], 500 pM (medium low QC), 1 nM (median QC), and 5 nM (high QC) for both compounds, with six replicates in each matrix. Because the drug concentration ranges in animal and clinical samples are likely to be higher than the upper limit of the calibration curve, extension of the dynamic range was evaluated by dilution. Human plasma spiked with 10, 50, and 200 nM GTI-2040 was diluted with 10% human plasma at 10-, 50-, and 200-folds, respectively ($n$ = 4). These standards were assayed, and dilution recovery was calculated by the dilution factors.

### Clinical Pharmacokinetic Studies of GTI-2040 on AML Patients

All clinical pharmacokinetic studies were performed under appropriate protocols in association with the Institutional Review Board (IRB) of The Ohio State University. GTI-2040 levels in plasma, RBC, and peripheral blood mononuclear cells (PBMC) were determined in 11 patients with AML following continuous intravenous infusion for a total of 144 h at a dose of 5 mg $kg^{-1}$ $day^{-1}$. Blood samples were collected at 0, 2, 4, 6, 12, 24, 48, and 72 h during infusion and at 0, 0.25, 0.5, 1, 2, 4, 6, 12, 24, and 48 h postinfusion. Plasma, PBMC, and RBC were separated from the whole blood using Vacutainer CPT tube (BD, San Diego, CA, USA) through a single centrifugation step according to the manufacturer's instruction. After collection of plasma, PBMC cells were carefully harvested. The cell membrane bound drug was removed by incubation with 0.2 mL of 0.1 μM PS-dC 28 on ice for 2 min, followed by PBS washing and gentle centrifugation. The cell number of PBMC was counted after the addition of trypan blue. PBMC and RBC cell lysates were prepared with addition of 200 μL of cell lysis buffer (10 mM Tris–HCl, pH 8.0, 0.5 mM EDTA, 1% Triton X-100). GTI-2040 concentrations in cell lysates were quantified using the ELISA method along with the plasma samples. Protein levels in PBMC cell lysate were determined with BCA assay (Pierce) and were used to normalize GTI-2040

**Table I.** Cutting Efficiency of S1 Nuclease at Levels of 60 and 100 U per Well

| Nominal template conc. (nM) | Cutting efficiency of S1 nuclease ($n$ = 5) | |
|---|---|---|
| | 60 U per well | 100 U per well |
| 50 | 99.3 ± 0.10% | 99.8 ± 0.03% |
| 100 | 99.6 ± 0.02% | 99.9 ± 0.01% |
| 200 | 99.7 ± 0.03% | 99.8 ± 0.01% |
| 250 | 99.7 ± 0.02% | 99.8 ± 0.01% |

concentration in PBMC (nanomolars per milligram protein). GTI-2040 in PBMC was converted to intracellular concentration (nanomolars) using a conversion factor of $2 \times 10^6$ cells to 1 μL cell volume or 1 μg protein to 0.035 μL cell volume.

## RESULTS

### Cutting Efficiency of S1 Nuclease as Evaluated by the One-Step Hybridization ELISA

Fluorescence response of the one-step capture ODN for GTI-2040 using a one-step hybridization ELISA was found to be linear from 0.025 to 50 nM. The cutting efficiency as estimated by Eq. (1) is shown in Table I. As shown, less than 1% of ODN remained intact after treatment of S1 nuclease at two levels, 60 and 100 U per well. Thus, based on this result, the cutting efficiency of S1 nuclease toward template ODN of GTI-2040 was nearly quantitative.

### Effect of S1 Nuclease on Selectivity of the Hybridization–Ligation ELISA

As shown in Fig. 1, the use of S1 nuclease in hybridization–ligation ELISA dramatically decreased the interference from the 3′N-1 putative metabolite without significant suppression of fluorescence signal on GTI-2040. Cross-reactivities of 3′N-1 metabolites on GTI-2040 were determined to be 89, 15, 11, 7.8, and 8.3% at levels of S1 nuclease 0, 15, 30, 60, and 100 U per well, respectively. At the same time, the maximum response of GTI-2040 decreased 2.2, 5, 7, and 11% with treatment of 15, 30, 60, and 100 U per well of S1 nuclease, respectively. The slight decrease in sensitivity for GTI-2040 was offset by a large gain in selectivity toward 3′N-1 metabolites. Because there was no further improvement in selectivity when 100 U per well of S1 nuclease was used, 60 U per well was chosen as the final concentration of S1 nuclease in the assay procedure. Additionally, further increase in S1 nuclease may destabilize the double-stranded DNA (manual of S1 nuclease, Invitrogen, Carlsbad, CA, USA). NaCl (100 mM) was found to stabilize both ends of double-stranded DNA toward attack by S1 nuclease (manual of S1 nuclease, Invitrogen) and was used as reaction buffer of S1 nuclease.

The use of S1 nuclease not only improved the assay selectivity, but also improved the linearity of the calibration curve of GTI-2040 below 10 nM. Figure 2 shows the fluorescence response of GTI-2040 at concentrations ranging from 0.1 to 10 nM at different levels of S1 nuclease. Good linearity was observed with S1 nuclease treatment. Without S1 nuclease treatment, GTI-2040 calibration curve was not linear even after addition of detergent. In such a case, a log–log transformation was necessary to generate linearity

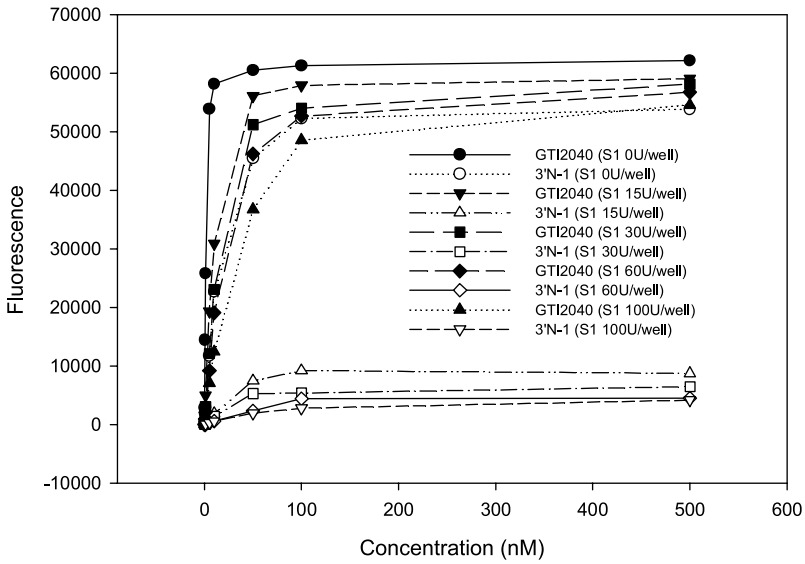


**Fig. 1.** Effect of S1 nuclease on assay selectivity. GTI-2040 or 3′N-1 (0.1 nM to 500 nM) was spiked in plasma followed by the hybridization–ligation ELISA without using S1 nuclease or using S1 nuclease at 15, 30, 60, and 100 U per well, respectively. Treatment of S1 nuclease decreased cross-reactivity of 3′N-1 dramatically from 89% without S1 nuclease to 15, 11,7.8, and 8.3% using 15, 30, 60, and 100 U per well S1 nuclease, respectively. Signal intensity of GTI-2040 only decreased 2.2, 5, 7, and 11% using 15, 30, 60, and 100 U per well S1 nuclease, respectively.

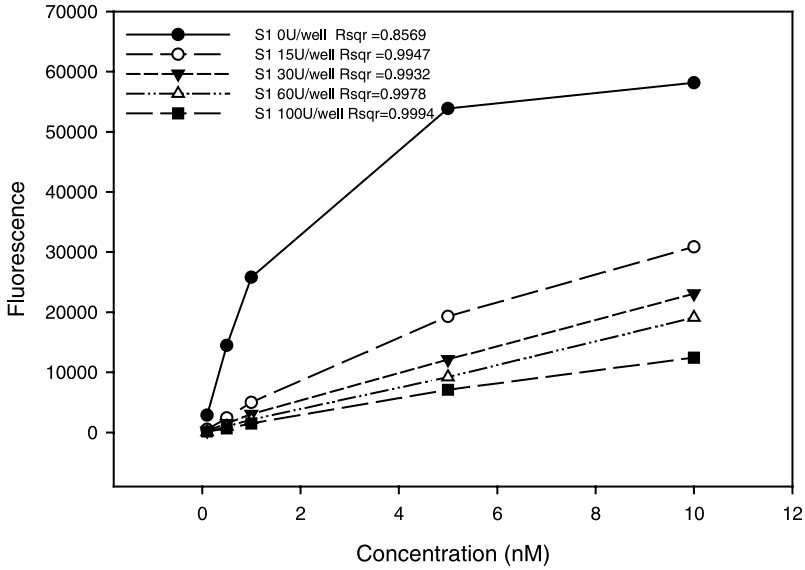


**Fig. 2.** Effect of S1 nuclease on linearity of GTI-2040 in plasma. Procedure of hybridization–ligation ELISA was followed. Treatment of S1 nuclease improved linearity of GTI-2040 as shown in concentration range from 0.1 to 10 nM.

(20,21). Another advantage of using S1 nuclease was the decrease in the background fluorescence. It was found that 60 U per well of S1 nuclease reduced background signal intensity to the noise levels generated from the microtiter wall. Effect of S1 nuclease on G3139 showed similar results as on GTI-2040 (data not shown).

## Optimization of the Hybridization ELISA Assays

Four key parameters, i.e., hybridization temperature, capture and probe ODN levels, and detergent, were identified as the major factors influencing assay sensitivity and accuracy and were optimized experimentally on G3139.

### *Hybridization Temperature*

Hybridization temperature in the first step is critical for selectivity and specificity of the assay. The effect of hybridization temperature on the signal intensity was evaluated for G3139. Because the hybridization temperature should be set 18–30°C below the Tm of G3139 (60°C), three temperatures (37, 42, and 50°C) were evaluated at different

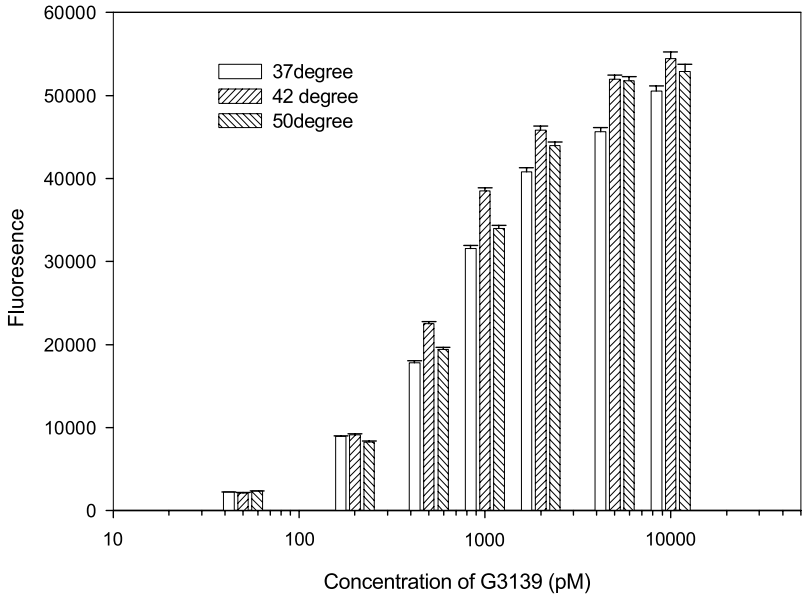


**Fig. 3.** Effect of hybridization temperature on the hybridization signal. Different temperatures (37, 42, and 50°C) were performed in the first hybridization step, and the second hybridization temperature was 18°C. At each level of G3139, fluorescence was highest at 42°C, and it was used as the hybridization temperature.

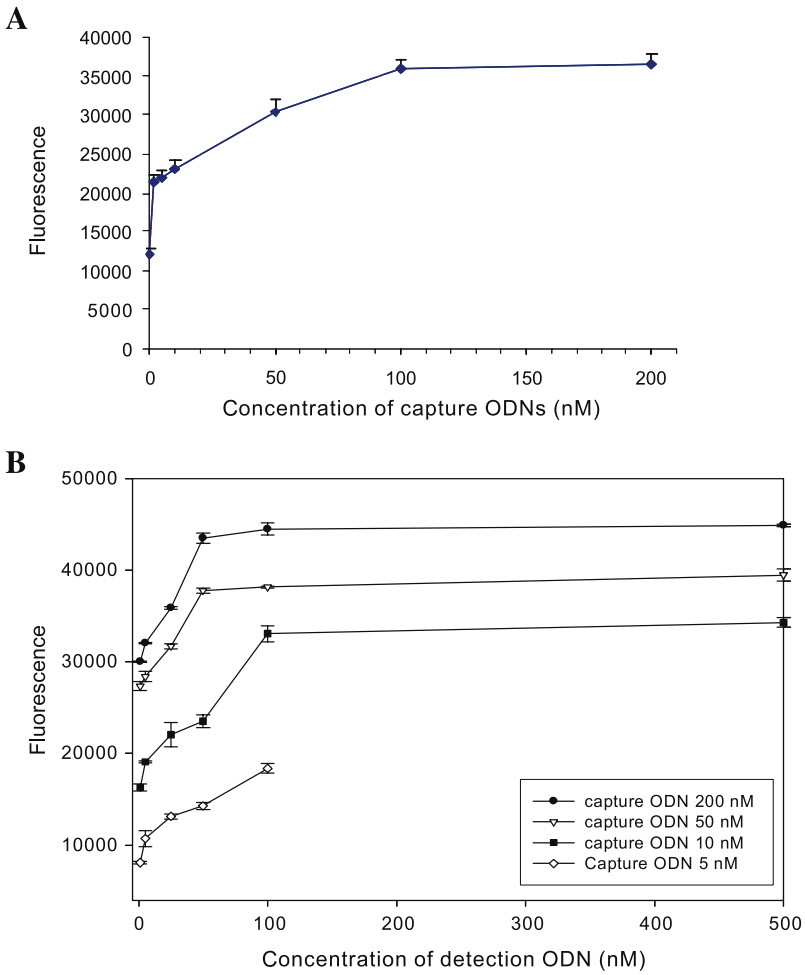


**Fig. 4.** Effect of capture and detection ODNs concentration on signal intensity. (A) Concentration of capture ODNs was changed, whereas the G3139 and detection ODN concentrations were fixed at 5 and 50 nM ($n$ = 3). (B) Detection ODN concentration varied at fixed G3139 concentration of 5 nM. Concentrations of capture ODNs were evaluated at 5, 10, 50, and 200 nM ($n$ = 3).

concentrations of G3139 for the signal intensity and linearity (Fig. 3). Linearity was not altered significantly at different temperatures (data not shown). Higher temperatures or stringent hybridization conditions reduced duplex formed by mismatched ODNs (e.g., four base mismatched ODN). However, temperature above 50°C compromised the binding of G3139 to the capture ODN, resulting in lower recovery and sensitivity. As shown in Fig. 3, we have found that the net fluorescence increased from 37 to 42°C, but decreased at higher temperatures. Therefore, we chose 42°C as the temperature in the first hybridization step.

The second hybridization step was not optimized using different temperatures because Tm of probe ODN is only 19.7°C. To maximize stability of detection probe–capture ODN duplex, incubation at 18°C overnight was used to ensure complete hybridization and ligation.

### *Capture and Detection Probe ODN Concentrations*

Capture ODN concentration is a critical variable for assay sensitivity and was optimized with G3139. Different

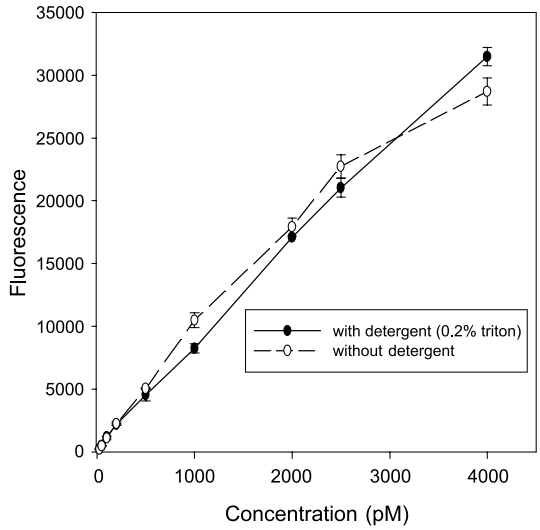


**Fig. 5.** Effect of detergent on assay linearity.

concentrations of capture ODN ranging from 0.2 to 200 nM were evaluated for the signal intensity with G3139 at 5 nM and with detection probe concentrations fixed at 50 nM. As concentrations of capture ODN increased from 0.2 to 10 nM, there was a sharp increase in fluorescence intensity (Fig. 4A). Above 10 nM, the fluorescence intensity only increased slowly until a plateau was reached at the capture ODN concentration of 200 nM. Therefore, capture ODN concentration of 200 nM was chosen to ensure the highest hybridization with analytes.

We also optimized the use of detection probe ODN by varying its concentration with the fixed G3139 concentration. Fluorescence intensity increased with an increased detection ODN level when the concentrations of capture ODN and G3139 were fixed, and a plateau was achieved at detection ODN concentration of about 100 nM (Fig. 4B). Further increase in detection ODN concentrations did not increase the signal intensity. Therefore, a detection ODN concentration of 100 nM was selected to preserve the quantity of probe ODNs. This combination of capture and detection ODNs concentration also offers good linearity and accuracy from 50 to 10,000 pM for GTI-2040 (data not shown).

*Effect of Detergent*

The effect of detergent on the assay characteristics is shown in Fig. 5. As shown, without detergent, the signal intensity exhibited saturation and linearity was poor. After addition of 0.25% Triton X-100, good linearity ($R^2$ = 0.997) was observed. For cell lysate, Triton X-100 at 1% was used to lyse cells, and signal was always linear with concentration from 25 to 5000 pM. Addition of detergent also improved the analyte recovery and hence the assay precision.

## Method Validation

*Specificity*

Potential interferences from endogenous matrix and from scrambled or mismatched oligonucleotides were first examined. The fluorescence responses from blank matrices evaluated were negligible and showed no difference from the PBS control. Scrambled GTI-2040 or reversed G3139, if present in the biological sample, did not seem to compete with the analytes in plasma as shown by their negligible fluorescence signal (Fig. 6). Mismatched ODNs that contain four mismatched nucleotides for GTI-2040 exhibited a cross-reactivity of only 5.77% (Table II). The slopes and intercepts of the calibration curves in 10 and 100% human plasma, 10% mouse plasma, 10% rat plasma, and cell lysates as shown in Fig. 7 were very close, indicating that the matrix effects were negligible for the hybridization ELISA assay.

*Cross-Reactivity with Chain-Shortened Metabolites*

Hybridization–ligation ELISA method demonstrated its selectivity toward the parent analyte from their putative 3′N-1 to 3′N-3 metabolites (Fig. 6). Compared to the concen-

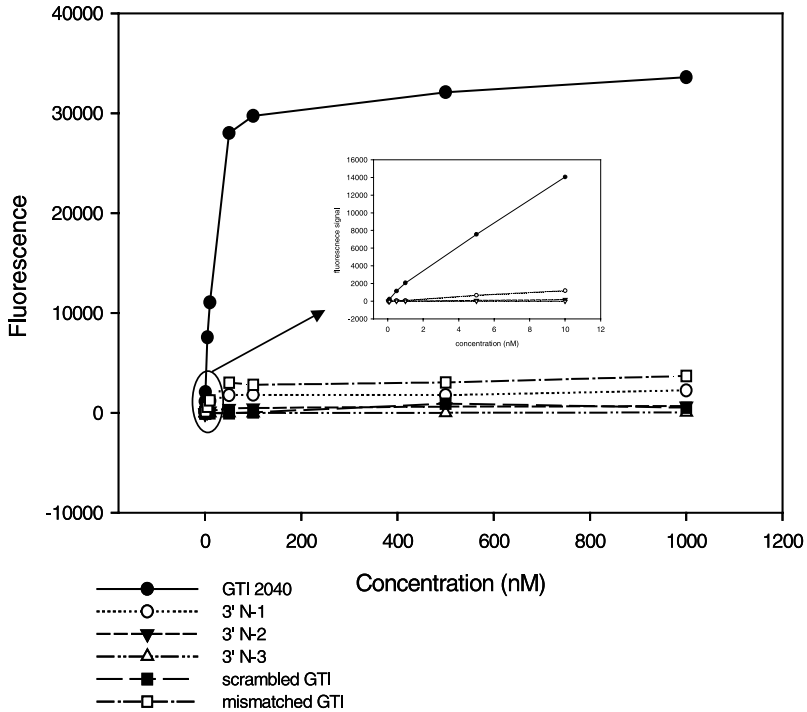


**Fig. 6.** Cross-reactivity of putative 3′-end metabolites (3′N-1, 3′N-2, and 3′N-3), and scrambled and mismatched GTI-2040. The small insert showed the cross-reactivity at low concentrations.

**Table II.** Cross-Reactivity of 3′- and 5′-End Putative Metabolites, and Mismatched and Scrambled ODNs Toward GTI-2040; and Cross-Reactivity of 3′N-1 of G3139 Toward G3139

| Name | Sequence (From 5′ to 3′) | Cross-reactivity (%) |
|---|---|---|
| GTI-2040 | GGCTAAATCGCTCCACCAAG | 100 |
| 3′N-1 | GGCTAAATCGCTCCACCAA | 5.9 |
| 3′N-2 | GGCTAAATCGCTCCACCA | 0.15 |
| 3′N-3 | GGCTAAATCGCTCCACC | 0.12 |
| 5′N-1 | GCTAAATCGCTCCACCAAG | 78.4 |
| Mismatched GTI-2040 | GGCTAAACTCGTCCACCAAG | 5.77 |
| Scrambled GTI-2040 | ACGCACTCAGCTAGTGACAC | <0.02 |
| G 3139 | TCT CCC AGC GTG CGC CAT | 100 |
| 3′N-1 of G3139 | TCT CCC AGC GTG CGC CA | 6.3 |

tration–response curve of parent ODNs, 3′N-1 to 3′N-3 metabolites of both GTI-2040 and G3139 all gave significantly lower fluorescence intensity. The cross-reactivity value for 3′N-1 G3139 was previously determined as 6.3% (10, Table II). The cross-reactivity value for 3′N-1 toward GTI-2040 was found to be 5.9% (Table II). For both GTI-2040 and G3139, a general trend shows that their cross-reactivities with 3′N-2 and 3′N-3 metabolites were lower than that with the 3′N-1 metabolites and were considered negligible (Table II). Because there is cross-reactivity of the assay with the 5′-deletion oligomers, this method is considered highly selective but not specific.

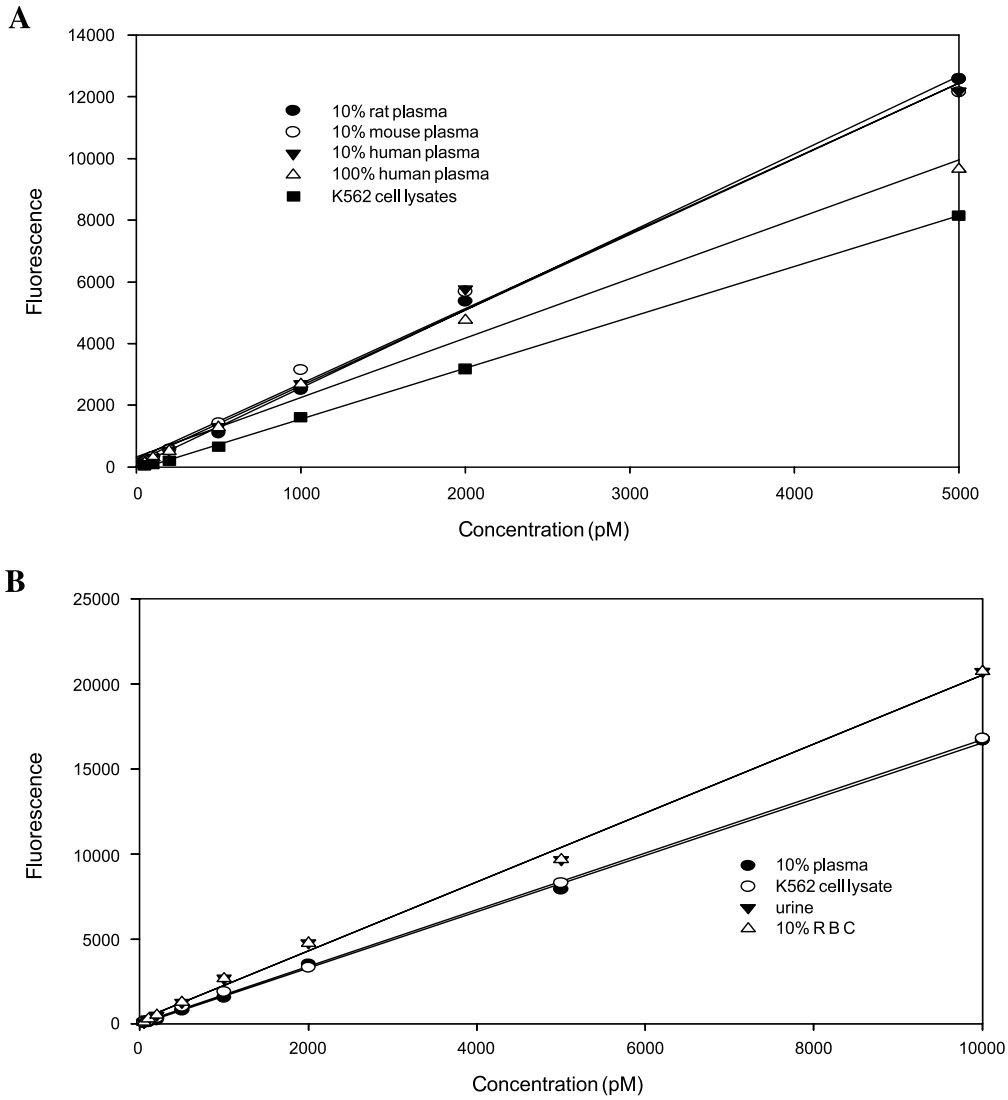


**Fig. 7.** Representative calibration curves of GTI-2040 in (A) 10% plasma from the rat, mouse, and human; 100% human plasma; and K562 cell lysates and (B) in human urine and 10% plasma, RBC, and K562 cell lysates.

**Table III.** Assay Accuracy and Reproducibility of GTI-2040 Plasma Samples Following Dilution

| Nominal concentration (nM) (dilution factor) | Mean measured concentration (nM) | Accuracy (%) | CV (%) |
|---|---|---|---|
| 10 (×10) | 10.54 | 105.4 | 6.6 |
| 50 (×50) | 55.18 | 110.4 | 6.5 |
| 200 (×200) | 226.3 | 113.3 | 7.1 |

*Linearity*

The hybridization–ligation ELISA was validated in a variety of biological matrices. The regression coefficients were all greater than 0.990. A lower limit of detection (LLOD; defined as five times signal to background noise) was found to be 25 pM and a lower limit of quantification (LLOQ) was found to be 50 pM for both G3139 and GTI-2040. As shown in typical calibration curves (Fig. 7), the assay was found to be linear from 50 to 10,000 pM for GTI-2040 and (50 to 5000 pM for) G3139. Beyond this range, fluorescence responses were found to reach a plateau in plasma or cell lysates. Therefore, 10 nM was set as the upper limit of the calibration curve for GTI-2040 and 5 nM for G3139. However, at concentrations ≥5 nM, serial dilution with 10% plasma in TE buffer could extend the dynamic range to 200 nM, and the effect of dilution on the accuracy and precision of the method was evaluated (Table III). The nominal accuracy values were 105.4, 110.4, and 113.3% at 10-, 50-, and 200-fold dilutions, respectively. Coefficients of variation (CVs) for each corresponding dilution factors were estimated as 6.6, 6.5, and 7.1%, respectively (Table III). These results indicated that the linear concentration range of the assay could be extended from 50 pM to 200 nM with acceptable precision and accuracy.

The within-day and between-day accuracy and precision of GTI-2040 in 10% human plasma, 100% human plasma, human red blood cell lysate (RBC), and K562 cell lysate are summarized in Table IV. The within-day precision (CV %) in human plasma at concentration levels of 100, 500, 1000, and 5000 pM were found to be 11.1, 7.4, 4.9, and 4.1% (all $n = 6$), respectively. The corresponding accuracy values were 103.1, 95.0, 95.7, and 101.5% (all $n = 6$) based on the nominal concentrations. The interday CVs were found to be 19.9, 12.9, 10.9, and 10.5%, respectively, with the corresponding accuracy values of 114, 93, 102.7, and 94.2% (all $n = 6$). The within-day CVs of the assay in K562 cell lysates were found to be 10.8, 2.3, 2.9, and 3.2% for the 100-, 500-, 1000-, and 5000-pM samples, respectively, with the corresponding accuracy values of 103.3, 103.5, 100.1, and 97.3% (Table IV). The validation data of the hybridization–ligation ELISA for G3139 were similar, and the between-run and within-run accuracy and precision have been reported previously (10).

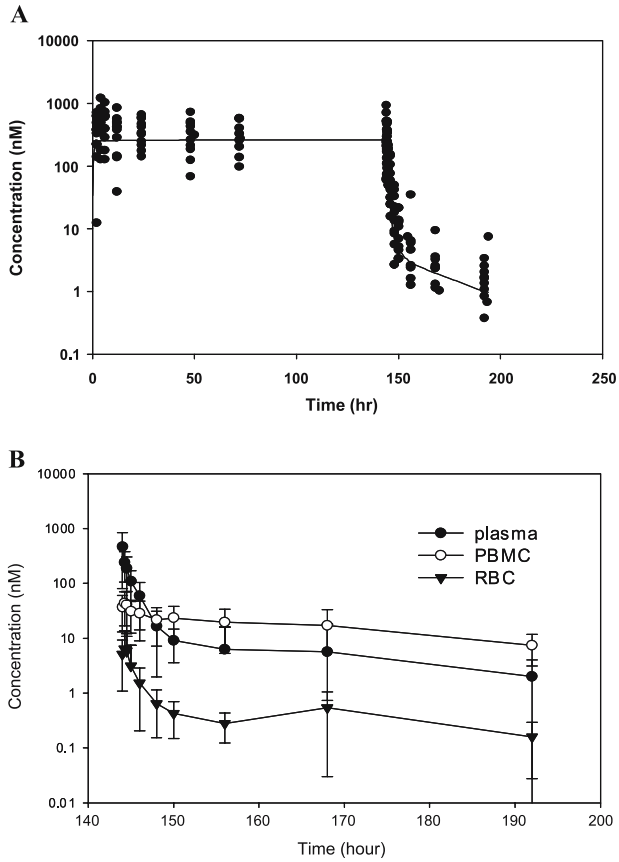


**Fig. 8.** (A) A composite plot of plasma concentration–time profiles of GTI-2040 in AML patients treated with i.v. infusion at a dose of 5 mg $kg^{-1}$ $day^{-1}$ for 144 h. Postinfusion profiles are shown up to 48 h ($n = 11$). (B) Expanded terminal concentration–time profiles of GTI-2040 in plasma, PBMC, and RBC. Plasma, RBC, and PBMC were obtained from 11 patients with AML following continuous i.v. infusion for 144 h at a dose of 5.0 mg $kg^{-1}$ $day^{-1}$.

## Application of the Hybridization–Ligation ELISA Assay *In Vivo*

This method was successfully used to characterize concentration–time profile of GTI-2040 in patients with

**Table IV.** Within-Day and Between-Day Accuracy and Reproducibility of GTI-2040 in Plasma; and Within-Day Accuracy and Precision in K562 Cell Lysates, RBC, and Urine

| GTI conc. Matrix | Accuracy (%) | | | | Reproducibility (CV %) | | | |
|---|---|---|---|---|---|---|---|---|
| | 100 pM | 500 pM | 1 nM | 5 nM | 100 pM | 500 pM | 1 nM | 5 nM |
| Plasma (within day) | 103.1 | 95 | 95.7 | 101.5 | 11.1 | 7.4 | 4.9 | 4.1 |
| Plasma (between day) | 114 | 93 | 102.7 | 94.2 | 19.9 | 12.9 | 10.9 | 10.5 |
| K562 | 103.3 | 103.5 | 100.1 | 97.3 | 10.8 | 2.3 | 2.9 | 3.2 |
| RBC | NA | 108.3 | 108.1 | 91.3 | NA | 5.7 | 6.9 | 4.9 |
| Urine | 98.4 | 92.3 | 100.9 | 96.4 | 18.7 | 5.1 | 11.5 | 7.4 |

**Table V.** Relevant Pharmacokinetic Parameters for GTI-2040 in AML Patients Given as an I.V. Infusion at 5 mg $kg^{-1}$ $day^{-1}$ for 144 h

| Parameters (unit) | Mean ± SD (or range) |
|---|---|
| $C_{ss}$ (nM) | 396.1 ± 200.1 |
| $(AUC_{0-\infty})$ (μM × h) | 54.0 ± 29.2 |
| CL (L $h^{-1}$) | 9.1 ± 6.4 |
| $V_{ss}$ (L) | 19.4 ± 15.6 |
| $V_1$(L) | 9.0 ± 6.8 |
| $(t_{1/2\alpha})$ (h) | 0.45 to 0.89 |
| $(t_{1/2\beta})$ (h) | 17.7 to 45.1 |
| $K_{21}$ (1 $h^{-1}$) | 0.032 ± 0.014 |
| MRT (h) | 1.95 ± 1.1 |

AML during and after the continuous i.v. infusion of GTI-2040 at a dose of 5 mg $kg^{-1}$ $day^{-1}$. Our assay was able to follow the plasma concentration–time course of GTI2040 until 48 h postdosing, which permitted the determination of accurate terminal half-life. The mean plasma concentration–time profile of GTI-2040 in patients showed a bi-exponential decline (Fig. 8A) and was well fitted to a two-compartment i.v. infusion model. As shown in Table V, the area under the concentration–time curve $(AUC_{0-\infty})$ was 54 ± 29 μM × h. The total body clearance (CL) value was 9.1 ± 6.4 L $h^{-1}$. The steady state volume of distribution ($V_{ss}$) was 19.4 ± 15.6 L. The mean initial half-life $(t_{1/2\alpha})$ was 0.71 h (0.45 to 0.89 h), and the mean terminal half-life $(t_{1/2\alpha})$ was 32 h (17.7 to 45.1 h). This is consistent with reports for other PS ODN antisense compounds, which generally gave an initial rapid decline followed by a sustained phase of elimination phase (20,26–31). Additionally, the ultrasensitivity of our assay allowed the determination of elimination phase of intracellular GTI-2040 concentrations in RBC and PBMC. As shown in Fig. 8B, RBC uptake of GTI-2040 was less than 5% but exhibited similar concentration–time profile as in plasma. In contrast, GTI-2040 concentrations in PBMC remained stable over time and were 2.7-fold higher than those in plasma postinfusion.

## DISCUSSION

Recently, several hybridization-based ELISA methods have been successfully developed for the determination of polynucleotides in biological matrices (10,19–25). Because of simplicity, we initially developed a one-step hybridization ELISA method on quantification of G3139 and GTI-2040 in biological matrix. Although good linearity was observed, the high cross-reactivity with the 3′-end metabolites precludes their practical uses. Herein, an ultrasensitive and selective hybridization–ligation ELISA was developed and validated for determination of GTI-2040 and G3139 in biological matrices including human plasma, PBMC, RBC, and cell lysates.

The hybridization ELISA is based on the Watson–Crick base-pairing and anti-Dig detection system, which provide high selectivity and sensitivity to the assay. To enhance the assay selectivity, especially the ability of discriminating from the 3′-end chain-shortened metabolites, a custom-designed 9-mer detection probe with its sequence complementary to the 5′ overhang of capture probe and 5′-end Dig-label was employed. In the presence of T4 ligase and ATP, ligation only occurs between the analyte and detection probe, forming well-bound duplexes (27-mer duplex for G3139 and 29-mer duplex for GTI-2040) that are detected by the Dig detection system. The 3′-end chain-shortened metabolites, when present, will bind to the capture probe but fail to complete ligation with detection probe due to their chain-shortened gap. The excess amount of capture probe would still bind to detection ODN, generating a short duplex, which will give signal and interfere with the assay. It was reported that $ddH_2O$ washing could remove unligated detection ODN (20). This is probably due to the higher binding affinity of the ligated analyte-detection probe complex with capture ODN (e.g., 29-mer), which has a 50°C difference in Tm values with the short duplex (9-mer). However, we have found that the unligated detection ODN could not be completely eliminated by washing only, which was evidenced by the poor linearity of GTI-2040 in plasma (Fig. 2) and its nonselectivity toward its 3′N-1 metabolite (89% cross-reactivity) (Fig. 1). Subsequently, we have found that after hybridization and ligation, incubation of the solution with S1 nuclease for 2 h at 37°C followed by the washing step dramatically reduced the background fluorescence and decreased the cross-reactivity with the 3′-end deletion metabolites (Fig. 1). S1 nuclease cuts single-strand region in DNA duplex with ≥99% efficiency (Table I) and single-strand region of an imperfectly formed DNA duplex, generating fragments that can be removed by washing. Therefore, cross-reactivity of GTI-2040 with its 3′N-1 metabolite was supposed to be minimal. We have also found that accessibility of S1 nuclease may be influenced by steric factors. In the one-step hybridization ELISA with GTI-2040, the cross-reactivity with 3′N-1 was 26%. This cross-reactivity value did not result from the background of the excess single-stranded capture probe because fluorescence from the control capture probe (without analyte) was minimal (<10%). We speculate that in the one-step hybridization ELISA, the bulky structure of digoxigenin next to the nick may pose steric hindrance for the S1 nuclease. In addition, in one-step hybridization ELISA, cross-reactivity with 3′N-2 and 3′N-3 metabolites were 18 and 10%, respectively, consistent with the lesser degree of steric hindrance with more nucleotides deletion from the 3′-end. On the other hand, in the hybridization–ligation ELISA, the single-strand regions in duplex were more open, facilitating the attack by the S1 nuclease. And we observed that the cross-reactivity of 3′N-1 dropped from 89 to 5.5% after using S1 nuclease in the two-step hybridization–ligation ELISA.

This possibility may also explain the high cross-reactivity with the 5′N-1 putative metabolite. The 5′-end deletion metabolites could still completely ligate with the detection probe with their intact 3′-end. On the other hand, the deleted region in the 5′end in the duplex, although could be cut by the S1 nuclease, may be difficult to remove due to the steric hindrance because the single-strand gap is located close to the plate wall. Therefore, the observed cross-reactivity with 5′N-1 was 78%. Fortunately, this cross reactivity may not pose a significant problem in practice because in biological samples, there were very few 5′-end metabolites detected for these two antisense compounds (32).

Our results also showed great improvement of linearity of GTI-2040 in plasma with addition of S1 nuclease as

illustrated in Fig. 2. Although the exact mechanism is not known, it may be attributed to the reduction in nonspecific background fluorescence signal. The overall evaluation led us to select 60 U per well of S1 nuclease as the working level in our study of these two oligonucleotides.

During the development of the one-step hybridization ELISA assay, it was found that the calibration curves in human and mouse plasma were not linear from 25 to 2500 pM, with lower-than-expected fluorescence signals at high concentrations. A log/log transformation improved the linearity and is commonly used for ELISA-based assays (20,25). We hypothesized that some plasma or cellular protein (possibly albumin) may interfere with the hybridization of antisense ODNs with capture ODNs at the first hybridization step, therefore causing nonlinearity. It was subsequently found that addition of 0.25% Triton X-100 (w/v) improved the assay linearity. Detergent is known to disrupt the nonspecific interaction between analyte and plasma protein, which may contribute to the nonlinearity. Additionally, disruption of the interaction between analyte and matrix not only extended the linear range to 5000 pM in plasma and cell lysate for both antisense compounds, but also improved the analyte recovery, thus the assay precision.

The validated hybridization–ligation ELISA method was previously applied to pharmacokinetic study of G3139 in phase I clinical trial (9) and for GTI-2040 in patients in the current study. In all instances, the ultrasensitivity of the ELISA assays allows a more accurate characterization of pharmacokinetics of these antisense compounds, especially the terminal half-lives and clearance values, when compared with the less sensitive HPLC method (11,12). For example, we were able to measure plasma concentration of GTI-2040 48 h after the end of drug infusion in AML patients and obtain a mean terminal half-life of more than 30 h. More importantly, this assay provided intracellular concentration–time profiles of GTI-2040 in PBMC and RBC obtained from AML patients, which showed sustained levels.

The assay format and procedure of hybridization–ligation ELISA described in this paper could possibly apply to general oligonucleotide antisense compounds in biological samples. For different oligonucleotides, it is necessary to design specific capture probe based on the sequence of the test antisense and a 9-mer overhang at 5′ terminal complementary to the sequence of the detection probe. Sequence design of the detection probe is based on two principles: (a) no similar match with the sequence of 5′overhang of the capture probe present for endogenous substances (the possible endogenous matches could be examined from BLAST database; http://www.ncbi.nlm.nih.gov/BLAST) and (b) as little base pairing occurs as possible between detection ODN and capture ODN in case detection probe shifts to the gap created by the chain-shortened metabolites. Poly A or other polynucleotides are the extreme examples resistant to the loss of base pairing resulting from frame-shift, and their use should be avoided. The sequence of detection probe ODNs does not have to be the same for different analytes because two different sequences for G3139 and GTI-2040 in terms of assay specificity or sensitivity worked equally well. However, poly A or other polynucleotides as detection probe ODNs are not recommended because we have found that these probes caused the assay to lose a single nucleotide resolution toward the 3′-end deletion oligomers (data not shown). When differentiation of 5′-end metabolites becomes necessary, the signal interference from 5′-end metabolites could be markedly reduced by using reversed sequence of capture and probe ODNs presented in this paper.

In conclusion, we have developed and validated a nonradioactive hybridization–ligation ELISA assay for determination of two antisense drugs, i.e., G3139 and GTI-2040, in a variety of biological matrices. The major advantages of this assay are: (a) ultrasensitive with an LLOQ of 50 pM, (b) highly selective toward 3′-end deletion metabolites, (c) negligible matrix effect, and (d) simple sample preparation and may be adapted to high throughput application. This assay has been successfully applied to measure plasma and intracellular levels of the two antisense drugs in clinics. With the design of appropriate capture and detection probes, this assay could be universally applicable in quantification of antisense compounds in a variety of biological matrices.

## ACKNOWLEDGMENTS

We acknowledge the support by NIH R21CA105879 and UO1 CA 76576.

## REFERENCES

1. P. J. Furdon, Z. Dominski, and R. Kole. RNase H cleavage of RNA hybridized to oligonulceotides containing methylphosphonate, phosphorothioate and phosphodiesterase bonds. *Nucleic Acids Res.* **17**:9193–9204 (1989).
2. R. Y. Walder and J. A. Walder. Role of RNase H in hybrid-arrested translation by antisense oligonucleotides. *Proc. Natl. Acad. Sci. USA* **85**:5011–5015 (1988).
3. I. Tamm, B. Dorken, and G. Hartmann. Antisense therapy in oncology: new hope for an old idea? *Lancet* **358**:489–497 (2001).
4. N. M. Dean and C. F. Bennett. Antisense oligonucleotide-based therapeutics for cancer. *Oncogene* **22**:9087–9096 (2003).
5. N. Dias and C. A. Stein. Antisense oligonucleotides: basic concepts and mechanism. *Mol. Cancer Ther.* **1**:347–355 (2002).
6. B. Jansen and U. Zangemeister-Wittke. Antisense therapy for cancer—the time for truth. *Lancet Oncol.* **3**:672–683 (2002).
7. Y. Lee, A. Vassilakos, N. Feng, V. Lam, H. Xie, H. Wang, M. Wang, H. Jin, K. Xiong, C. Liu, J. Wright, and A. Young. GTI-2040, an antisense agent targeting the small subunit component (R2) of human ribonucleotide reductase, shows potent antitumor activity against a variety of tumors. *Cancer Res.* **63**:2802–2811 (2003).
8. A. A. Desai, R. L. Schilsky, A. Young, L. Janisch, W. M. Stadler, N. J. Vogelzang, S. Cadden, J. A. Wright, and M. J. Ratain. A phase I study of antisense oligonucleotide GTI-2040 given by continuous intravenous infusion in patients with advanced solid tumors. *Ann. Oncol.* **16**:958–965 (2005).
9. G. Marcucci, W. Stock, G. Dai, R. B. Klisovic, S. Liu, M. I. Klisovic, W. Blum, C. Kefauver, D. A. Sher, M. Green, M. Moran, K. Maharry, S. Novick, C. D. Bloomfield, J. A. Zwiebel, R. A. Larson, M. R. Grever, K. K. Chan, and J. C. Byrd. Phase I study of oblimersen sodium, an antisense to Bcl-2, in untreated older patients with acute myeloid leukemia: pharmacokinetics, pharmacodynamics, and clinical activity. *J. Clin. Oncol.* **23**:3404–3411 (2005).
10. G. Dai, K. K Chan, S. Liu, D. Hoyt, W. Whitman, M. Klisovic, T. Shen, M. A. Caligiuri, J. Byrd, M. Grever, and G. Marcucci. Cellular uptake and intracellular levels of the bcl-2 antisense g3139 in cultured cells and treated patients with acute myeloid leukemia. *Clin. Cancer Res.* **11**:2998–3008 (2005).
11. A. J. Bourque and A. S. Cohen. Quantitative analysis of

phosphorothioate oligonucleotide in biological fluids using fast anion-exchange chromatography. *J. Chromatogr.* **617**:43–49 (1993).
12. S. T. Crooke, M. J. Graham, J. E. Zuckerman, D. Brooks, B. S. Conklin, L. L. Cummins, M. J. Greig, C. J. Guinosso, D. Kornbrust, M. Manoharan, H. M. Sasmor, T. Schleich, K. L. Tivel, and R. H. Griffey. Pharmacokinetics properties of several novel oligonucleotide analogs in mice. *J. Pharmacol. Exp. Ther.* **277**:923–937 (1996).
13. R. H. Griffey, M. J. Greig, H. J. Gaus, K. Liu, D. Monteith, M. Winniman, and L. L. Cummins. Characterization of oligonucleotide metabolism in vivo via liquid chromatography/electrospray tandem mass spectrometry with a quadrupole ion trap mass spectrometer. *J. Mass Spectrom.* **32**:305–313 (1997).
14. H. L. Gaus, S. R. Owens, M. Winniman, S. Cooper, and L. L. Cummins. On-line HPLC electrospray mass spectrometry of phosphorothioate oligonucleotide metabolites. *Anal. Chem.* **69**:313–319 (1997).
15. J. C. Bres, F. Morvan, I. Lefebvre, J. J. Vaseur, A. Pompon, and J. L. Imbach. Kinetics study of the biotransformation of an oligonucleotide prodrug in ells extract by matrix-assisted laser desorption-ionization time-of-flight mass spectrometry. *J. Chromatogr. B Biomed. Sci. Appl.* **753**:123–130 (2001).
16. S. H. Chen and J. M. Gallo. Use of capillary electrophoresis methods to characterize the pharmacokinetics of antisense drugs. *Electrophoresis* **19**:2861–2869 (1998).
17. P. A. Cossum, H. Sasmor, D. Dellinger, L. Truong, and L. Cmunnins *et al.* Disposition of the 14C-labeled phosphorothioate oligonucleotide ISIS 2105 after intravenous administration to rats. *J. Pharmacol. Exp. Ther.* **267**:1181–1190 (1993).
18. F. I. Raynaud, R. M. Orr, P. M. Goddard, H. A. Lacey, and H. Lancashire *et al.* Pharmacokinetics of G3139, a phosphorothioate oligodeoxynucleotide antisense to bcl-2, after intravenous administration or continuous subcutaneous infusion to mice. *J. Pharmacol. Exp. Ther.* **281**:420–427 (1997).
19. R. Z. Yu, R. S. Geary, and A. A. Levin. Application of novel quantitative bioanalytical methods for pharmacokinetic and pharmacokentic/pharmacodynamic assessments of antisense oligonucleotides. *Drug Discov. Dev.* **7**:195–203 (2004).
20. R. Z. Yu, B. Baker, A. Chappell, R. S. Geary, E. Cheung, and A. A. Levin. Development of an ultrasensitive noncompetitive hybridization–ligation enzyme-linked immunosorbent assay for the determination of phosphorothioate oligodeoxynucleotide in plasma. *Anal. Biochem.* **304**:19–25 (2002).
21. J. R. Deverre, V. Boutet, D. Boquet, E. Ezan, J. Grassi, and J. M. Grogent. A competitive enzyme hybridization assay for plasma determination of phosphodiester and phosphorothioate antisense oligonucleotides. *Nucleic Acids Res.* **25**:3584–3589 (1997).
22. S. M. Efler, L. Zhang, B. O. Noll, E. Uhlmann, and H. L. Davis. Quantification of oligodeoxynucleotides in human plasma with a novel hybridization assay offers greatly enhanced sensitivity over capillary gel electrophoresis. *Oligonucleotides* **15**:119–131 (2005).
23. M. Serresde, M. J. McNulty, L. Christensen, G. Zon, and J. W. Findlay. Development of a novel scintillation proximity competitive hybridization assay for the determination of phosphorothioate antisense oligonucleotide plasma concentrations in a toxicokinetic study. *Anal. Biochem.* **233**:228–233 (1996).
24. K. L. Sewell, R. S. Geary, B. F. Baker, J. M. Glover, T. G. Mant, R. Z. Yu, J. A. Tami, and F. A. Dorr. Phase I trial of ISIS 104838, a 2′-methoxyethyl modified antisense oligonucleotide targeting tumor necrosis factor-α. *J. Pharmacol. Exp. Ther.* **303**:1334–1343 (2002).
25. P. Brown-Augsburger, X. M. Yue, J. A. Lockridge, J. A. McSwiggen, D. Kamboj, and K. M. Hillgren. Development and validation of a sensitive, specific, and rapid hybridization-ELISA assay for determination of concentrations of a ribozyme in biological matrices. *J. Pharm. Biomed. Anal.* **34**:129–139 (2004).
26. R. S. Geary, J. M. Leeds, J. Fitchett, T. Burckin, and L. Truong *et al.* Pharmacokinetics and metabolism in mice of a phosphorothioate oligonucleotide antisense inhibitor of C-raf-1 kinase expression. *Drug Metab. Dispos.* **25**:1272–1281 (1997).
27. R. Zhang, J. Yan, H. Shahinian, G. Amin, Z. Lu, and T. Liu *et al.* Pharmacokinetics of an anti-human immunodeficiency virus antisense oligodeoxynucleotide phosphorothioate (GEM 91) in HIV-infected subjects. *Clin. Pharmacol. Ther.* **58**:44–53 (1995).
28. R. Z. Yu, R. S. Geary, J. M. Leeds, T. Watanabe, and M. Moore *et al.* Comparison of pharmacokinetics and tissue disposition of an antisense phosphorothioate oligonucleotide targeting human Ha-ras mRNA in mouse and monkey. *J. Pharm. Sci.* **90**:182–193 (2001).
29. M. J. Morris, W. P. Tong, C. Cordon-Cardo, M. Drobnjak, and W. K. Kelly *et al.* Phase I trial of BCL-2 antisense oligonucleotide (G3139) administered by continuous intravenous infusion in patients with advanced cancer. *Clin. Cancer Res.* **8**:679–683 (2002).
30. D. A. Brown, S. H. Kang, S. M. Gryaznov, L. Dedioniso, O. Heidenreich, S. Sullivan, X. Xu, and M. I. Nerenberg. Effect of phosphorothioate modification of oligodeoxynucleotides of specific protein binding. *J. Biol. Chem.* **269**:26801–26805 (1994).
31. A. A. Levin. A review of the issues in the pharmacokinetics and toxicology of phosphorothioate antisense oligonucleotides. *Biochim. Biophys. Acta* **1489**:69–84 (1999).
32. G. Dai, X. Wei, Z. Liu, S. Liu, G. Marcucci, and K. K. Chan. Characterization and quantification of Bcl-2 antisense G3139 and metabolites in plasma and urine by ion-pair reversed phase HPLC coupled with electrospray ion-trap mass spectrometry. *J. Chromatogr. B* **825**:201–213 (2005).